3-1-2020

Amplification of explosive width in complex networks

Pitambar Khanra
National Institute of Technology, Durgapur

Prosenjit Kundu
National Institute of Technology, Durgapur

Pinaki Pal
National Institute of Technology, Durgapur

Peng Ji
Fudan University

Chittaranjan Hens
Indian Statistical Institute, Kolkata

Follow this and additional works at: https://digitalcommons.isical.ac.in/journal-articles

Recommended Citation

Amplification of explosive width in complex networks

Pitambar Khanra, Prosenjit Kundu, Pinaki Pal, et al.

View Online   Export Citation   CrossMark

ARTICLES YOU MAY BE INTERESTED IN

Amplification of explosive width in complex networks

Pitambar Khanra,[1] (ID) Prosenjit Kundu,[1] (ID) Pinaki Pal,[1] Peng Ji,[2] (ID) and Chittaranjan Hens[3,a] (ID)

AFFILIATIONS

[1] Department of Mathematics, National Institute of Technology, Durgapur 713209, India
[2] The Institute of Science and Technology for Brain-inspired Intelligence, Fudan University, Shanghai 200433, China
[3] Physics and Applied Mathematics Unit, Indian Statistical Institute, Kolkata 700108, India

[a] Author to whom correspondence should be addressed: chittaranjanhens@gmail.com

ABSTRACT

We present an adaptive coupling strategy to induce hysteresis/explosive synchronization in complex networks of phase oscillators (Sakaguchi–Kuramoto model). The coupling strategy ensures explosive synchronization with significant explosive width enhancement. Results show the robustness of the strategy, and the strategy can diminish (by inducing enhanced hysteresis loop) the contrarian impact of phase frustration in the network, irrespective of the network structure or frequency distributions. Additionally, we design a set of frequency for the oscillators, which eventually ensure complete in-phase synchronization behavior among these oscillators (with enhanced explosive width) in the case of adaptive-coupling scheme. Based on a mean-field analysis, we develop a semi-analytical formalism, which can accurately predict the backward transition of the synchronization order parameter.

The phenomenon of synchronization has fascinated researchers for many years due to its appearance in a variety of natural as well as manmade systems. However, the study of synchronization in adaptively coupled complex networks has got less attention. Here, we have presented an adaptive coupling scheme and explored the impact of that in the enhancement of explosive width in the Sakaguchi–Kuramoto model on complex networks. Numerical investigation shows that the proposed scheme ensures explosive synchronization (ES) with significant explosive width enhancement for diverse frequency distributions with different network realizations. More importantly, it is found that the proposed coupling scheme can inhibit the contrarian impact of the phase frustration in the network. We also have established a semi-analytical treatment for investigating the system using the Ott–Antonsen ansatz. The results obtained from the semi-analytical approach are found to match closely with the numerical simulation results. The analysis shows that the adaptive-coupling function is robust and can enhance the hysteresis width in different complex networks having a variety of natural frequency distributions and for a broad range of frustration parameters.

I. INTRODUCTION

Adaptively coupled oscillators have been found to exhibit a wide range of complex behaviors.[1–4] For instance, link weights co-evolving with underlying dynamics can enhance synchronizability in heterogeneous networks,[5] and this mechanism can induce spontaneous synchronization in, e.g., certain groups of neurons of a brain by adjusting the adaptive Hebbian learning process.[6–9] Recently, it has been reported that the adaptation of the coupling configuration by the local order parameter may result in explosive synchronization, a phenomenon characterized by discontinuous (first-order) phase transitions between incoherent and coherent states accompanied by hysteresis in networks of coupled oscillators.[10–17]

Of particular interest, explosive synchronization[18,19] has been found to emerge among adaptively coupled oscillators irrespective of the structure of the networks or intrinsic frequency distributions. We now raise the question "what happens if we use a modified strategy obtained by incorporating higher power of the adapting parameter?" Here, we use a modified adaptive-coupling scheme proposed by Filatrella et al.[18] on the Sakaguchi–Kuramoto model in a complex network environment, and results show that the proposed scheme can amplify or increase the hysteresis width (difference

between the backward transition and forward transition points of synchronization) for diverse frequency distributions with different network realizations. For demonstration, we start with the classical network-coupled Sakaguchi–Kuramoto phase oscillators of size N.[20–23] Dynamics of each oscillator in the network is governed by the equation

$$\frac{d\theta_i}{dt} = \omega_i + \lambda l_i \sum_{j=1}^{N} A_{ij} \sin(\theta_j - \theta_i - \alpha), \quad (1)$$

where ω_i is the intrinsic natural frequency of the ith oscillator and A_{ij} is an ijth element of the adjacency matrix $A = (A_{ij})_{N \times N}$.

Here, α accounts for a frustrating term within the range of $0 \leq \alpha < \frac{\pi}{2}$ [24–28] and λ is the coupling strength. l_i is a time-dependent coupling term and contributes adiabatically to the coupling function.

As a general choice, we consider l_i as a function of the Kuramoto order parameter R, which quantifies the degree of synchronization of the entire population. The global order parameter is defined as

$$R e^{i(\psi - \alpha)} = \frac{1}{N} \sum_{j=1}^{N} e^{i(\theta_j - \alpha)}, \quad (2)$$

where $0 \leq R \leq 1$ quantifies the magnitude of coherence and ψ denotes the average phase. Prior research has shown that the adaptive function $l_i = R$ can result in explosive synchronization.[10,19] However, this strategy generates a constant hysteresis or explosive width. We seek here a suitable choice of l_i which can enhance the hysteresis loop of phase-coupled networks and choose the adaptive function as $l_i = R^{z-1}$, where $z \, (\geq 1)$ is a positive real number.[18]

To illustrate the effectiveness of our choice, we consider a heterogeneous Erdős–Rényi (ER) network with $N = 3 \times 10^2$ nodes. We increase (decrease) the coupling strength λ adiabatically with an increment (decrement) $\delta\lambda = 0.01$ and compute the stationary value of R for each λ during the forward (backward) transition from the incoherent to the phase synchronized state. In this simulation, we take the natural frequencies from a Lorentzian distribution and set the frustration parameter (α) equal to 0.5. In Fig. 1(a), the order parameter undergoes a continuous transition for the choice of $z = 1$ where the network is purely diffusive, i.e., the coupling function is not controlled by any adaptive coupling. However, setting the adaptive parameter to a higher power ($z = 2$), one can generate a discontinuous (explosive) transition in the synchronization order parameter [see Fig. 1(b)]. Interestingly, the explosive width is further enhanced if we increase the value of z from 2 to 3 [Fig. 1(c)]. The double headed arrow in Fig. 1(c) indicates the explosive width for the explosive synchronization transition, which is the difference between the backward transition and forward transition points of synchronization. In this paper, we have explored the impact of z on the transition to synchronization in different complex networks of Sakaguchi–Kuramoto oscillators for a broad range of frequency distributions, namely, Lorentzian or uniform distributions. We have also considered the degree-frequency correlated environment and a special form of degree-frequency correlation, which eventually gives perfect synchronization. Our results show that the adaptive coupling function is robust and can induce the enhanced explosive width for a broad range of frustration parameter over diverse network settings. In this work, we validate our detailed numerical results by solving a (semi-analytically) order parameter equation on the basis of Ott–Antonsen ansatz.[29] The
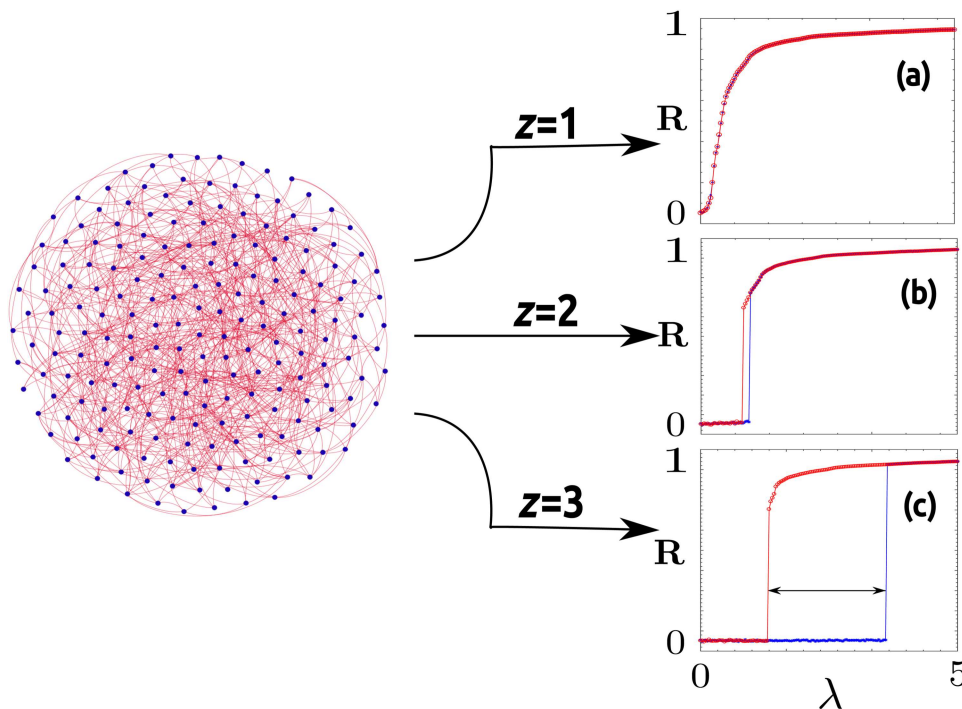
FIG. 1. Expansion of hysteresis width in small network. Visualization of the expansion of the hysteresis width for an ER network of size $N = 300$, $\langle k \rangle = 12$ with increasing z. The right panel synchronization diagram is constructed using the model equation (1) with phase-frustration value $\alpha = 0.5$. The double headed arrow in (c) indicates explosive width of the synchronization transition.

forward transition curve is perfectly fitted with our semi-analytical findings.

II. ANALYTICAL APPROACH AND NUMERICAL VERIFICATION

We start with the *annealed network* approximation proposed in Refs. 30–34, which gives critical behavior of phase transitions (including synchronization transition) in complex networks. For the case of a sparse uncorrelated complex network with a degree distribution $P(k)$ in the thermodynamic limit ($N \to \infty$), we may write

$$\frac{d\theta_i}{dt} = \omega_i + \frac{\lambda R^{z-1} k_i}{N \langle k \rangle} \sum_{j=1}^{N} k_j \sin(\theta_j - \theta_i - \alpha), \tag{3}$$

where k_i is the degree of ith node and $\langle k \rangle$ is the average degree across nodes. To obtain the explicit set of equations for the time evolution of the complex order parameter $C = Re^{i(\psi - \alpha)}$, we use here the Ott–Antonsen ansatz,[29] where the density of the oscillators at time t with phase θ for a given degree k and frequency ω be given by the function $f(k, \omega; \theta, t)$, and we normalize it as

$$\int_0^{2\pi} f(k, \omega; \theta, t) d\theta = h(k, \omega) = P(k)g(\omega). \tag{4}$$

To maintain the conservation of the oscillators[20,31] in a network, the density function f satisfies the continuity equation

$$\frac{\partial}{\partial t} f(k, \omega; \theta, t) + \frac{\partial}{\partial \theta} [vf(k, \omega; \theta, t)] = 0, \tag{5}$$

where v is the velocity field on the circle that drives the dynamics of f, which comes from the right-hand side of Eq. (3) as follows:

$$v(k, \omega; \theta, t) = \frac{d\theta}{dt} = \omega + \frac{\lambda k}{2i} R^{z-1} \left[Ce^{-i\theta} - C^* e^{i\theta} \right]. \tag{6}$$

Expanding $f(k, \omega; \theta, t)$ in a Fourier series in θ, we have

$$f = \frac{h(k, \omega)}{2\pi} \left\{ 1 + \left[\sum_{n=1}^{\infty} f_n(k, \omega, t) e^{in\theta} + \text{c.c.} \right] \right\}, \tag{7}$$

where c.c. stands for the complex conjugate. We now consider the Ott–Antonsen ansatz

$$f_n = \beta^n(k, \omega, t) \tag{8}$$

to obtain an equation for the function $\beta(k, \omega, t)$ and find the following equation:

$$\frac{\partial \beta}{\partial t} + i\omega\beta + \frac{\lambda k}{2} R^{z-1}(C\beta^2 - C^*) = 0, \tag{9}$$

where $|\beta(k, \omega, t)| \leq 1$ to avoid the divergence of the series. The above equation is not yet in a closed form. So, to make the above equation in a closed form, we get the complex global order parameter as

$$C(t) = \frac{e^{-i\alpha}}{\langle k \rangle} \int_{k_{min}}^{\infty} \int_{-\infty}^{\infty} kP(k)g(\omega)\beta^* d\omega \, dk. \tag{10}$$

Now, to study a steady state solution, we average $C(t) = Re^{i\psi - i\alpha + i\Omega t}$ for the constant order parameter R, a phase ψ, and a group angular velocity Ω. By suitably varying the reference frame, $\omega \mapsto \omega - \Omega$ and putting $\psi = 0$, without loss of generality, we have $C = Re^{-i\alpha}$. Therefore, $C^* = Re^{i\alpha}$ and for stationary points of Eq. (9) we find the solution of $\dot{\beta} = 0$.

We obtain the solution as follows:

$$\beta(k, \omega) = \begin{cases} -ixe^{i\alpha} + e^{i\alpha}\sqrt{1 - x^2}, & |x| \leq 1, \\ -ixe^{i\alpha} \left[1 - \sqrt{1 - \left(\frac{1}{x}\right)^2} \right], & |x| > 1, \end{cases} \tag{11}$$

where $x = \frac{\omega - \Omega}{\lambda kR^z}$ and this solution satisfies the requirement $|\beta| \leq 1$ for the convergence of the geometrical series [Eq. (8)]. The first solution corresponds to the synchronous state, and the second solution is due to the desynchronous state. In this case, the order parameter can be rewritten as

$$R = \frac{1}{\langle k \rangle} \left[\int \int_{k_{min}}^{\infty} kP(k)g(\omega)\beta^*(k, \omega)H(1 - |x|) \, dk \, d\omega \right. $$
$$\left. + \int \int_{k_{min}}^{\infty} kP(k)g(\omega)\beta^*(k, \omega)H(|x| - 1) \, dk \, d\omega \right], \tag{12}$$

where H is Heaviside functions. The first part of the right-hand side of Eq. (12) encompasses the contribution of locked oscillators, and the second part accounts for the contribution of drift oscillators to the order parameter R. Splitting the contributions of real and imaginary parts, we can eventually obtain the coupled self-consistent equations of R and Ω (see the Appendix).

To test the impact of z on the transition to synchronization, we use a heterogeneous scale-free network ($N = 2000$, $\langle k \rangle = 12$, and $\gamma = 2.8$) generated from the configuration model, the frequencies are drawn from a Lorentzian distribution with a mean of 0 and a standard deviation of 1. The bi-stable state (hysteresis regime) is shown by the yellow color (regime: II) in Figs. 2(a) and 2(b) for the frustration parameters $\alpha = 0.0$ and $\alpha = 0.5$, respectively. For lower z, the hysteresis width is found to be negligibly small and if we increase this adaptive parameter to higher values, the width is significantly enhanced irrespective of the frustration parameter. Here, the magenta island (regime: I) shows the de-synchronized regime, and cyan island (regime: III) is the locked part of coupled phase oscillators. It is observed from the figure that as z is increased, the region of the hysteresis is amplified significantly. Interestingly, the higher adaptive-coupling parameter ($z > 1$) not only induces explosive synchronization in the network but also enhances the explosive width even for high phase frustration [e.g., $\alpha = 0.5$ in Fig. 2(b)]. Typically, higher phase frustration ($\alpha > 0.3$) destroys the hysteresis behavior in a degree-frequency correlated network when $z = 1$.[34] However, for a higher value of z, it can overcome the situation and explosive synchronization (ES) re-emerges, a study never explored before. The boundary of the yellow and cyan regions which signifies the forward critical point [$\lambda_f(z)$] of the hysteresis transition is computed numerically from the model equation (1). The backward transition points computed from the self-consistent coupled equations of R and Ω (see the Appendix) are shown with black diamonds
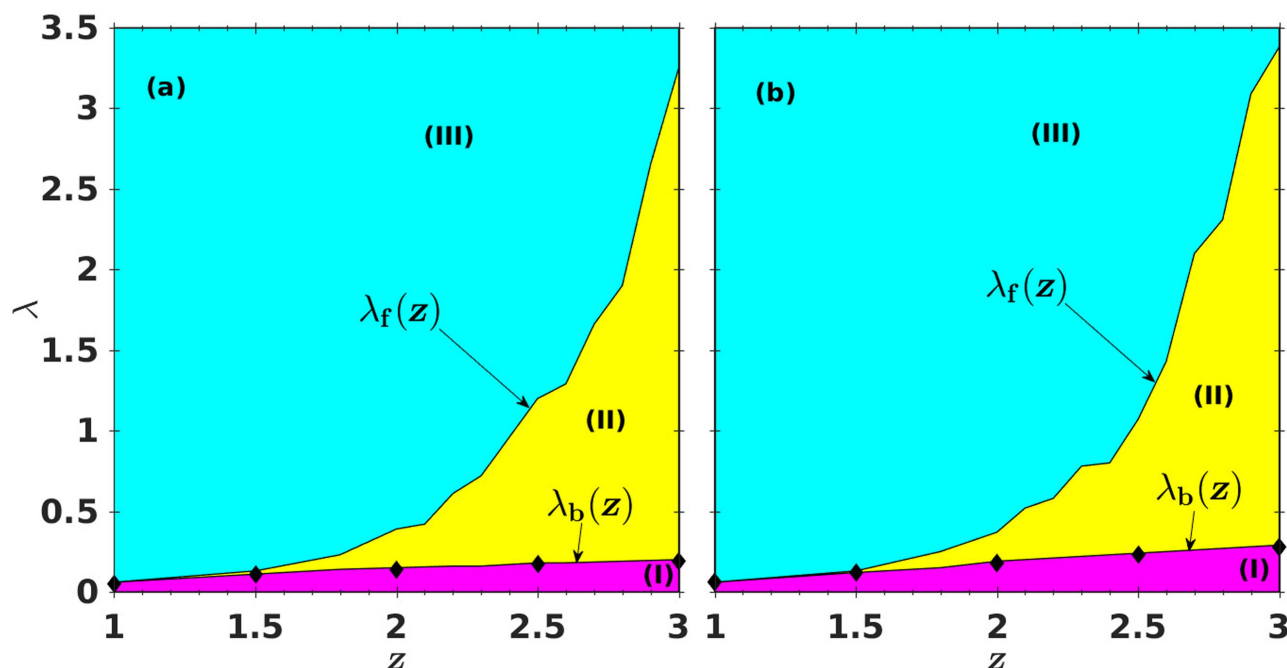
FIG. 2. Phase diagram on the $z - \lambda$ plane showing the amplification of hysteresis width. Magenta (I), yellow (II), and cyan (III) islands, respectively, represent asynchronous ($R \sim 0$), hysteresis, and synchronous ($R \sim 1$) regions. These regions are separated by solid black lines indicating the critical coupling strength for the transition to synchrony during the forward (λ_f) and backward (λ_b) continuations. Both the figures are constructed with a scale-free (SF) network of size $N = 2000$, $\langle k \rangle = 12$, and $\gamma = 2.8$. Panel (a) indicates zero phase frustration, i.e., $\alpha = 0$ and panel (b) indicates $\alpha = 0.5$. The solid black boundary separating regions (II) and (III) and solid line separating regions (I) and (II) have been obtained from numerical simulation. The black diamonds on this line are obtained from the semi-analytical approach [Eqs. (A3) and (A4)].

in Fig. 2, which show a close match with the solid black boundary separating magenta and yellow regions obtained from numerical simulation.

We have also numerically calculated the order parameter and the global frequency Ω for $z = 2$ and $z = 3$ (see Fig. 3). The order parameter (R) and global frequency (Ω) are shown in Figs. 3(a) and 3(c) with blue lines and Figs. 3(b) and 3(d) with red lines, respectively, as a function of λ. The backward transition points determined from the self-consistent equations are shown with dashed vertical lines in the figure, which shows a very close match with the backward points obtained through numerical simulation of the whole system. For $z = 2$, the hysteresis width [see the inset of Figs. 3(a) and 3(b)] occurs due to the presence of adaptive coupling. For $z = 3$, the width is significantly enhanced compared to $z = 2$. Note that, the values of Ω and R are negligibly small before the forward critical coupling. The reason is as follows: adaptive function $R^{(z-1)}$, acting on each node of the network, decreases the effective coupling ($\Lambda_{eff} = \lambda \times R^{(z-1)}$ where $0 < R < 1$ and $z > 1$) substantially. Therefore, higher strength is required to establish a locked phase. Numerical values of backward R and Ω closely match with the ones obtained from the semi-analytical expression of R and Ω derived from Eq. (12).

For further validation of the scheme presented here, we simulate the model [Eq. (1)] using a Watts–Strogatz small-world

network ($N = 5 \times 10^2$, $\langle k \rangle = 4$, and with a rewiring probability $\beta = 0.5$). We have checked the impact of z in three different values of $\alpha = 0, 0.3$, and 0.6. In the left panel of Fig. 4, the ES and the enhancement of explosive width (double headed arrow) for three z values ($z = 1$ in green, $z = 2$ in blue, and $z = 3$ in red line) are shown for $\alpha = 0$. In the middle panel and the right panel, α values are fixed at 0.3 and 0.6, respectively. We, therefore, observe that the tuning parameter appearing as a power in the adaptive term can enhance the width of hysteresis for a large class of networks and for a wide range of phase frustration.

We perform the numerical analysis for a diverse set of frequency distributions, and we show that the enhancement properties appear for all the cases which only depend on z. The changes in forward and backward points depend on the choices of frequency distributions. Next, we validate our proposition in frustrated networks for a certain choice of frequency distribution directly correlated with its own degree in which a global order parameter achieves *perfect synchronization*[35] ($R = 1$). This is important, as z mainly contributes to the enhancement of hysteresis width irrespective of α. Although α frustrates the system by not allowing the order parameter to reach perfect synchronization, we seek a selection of frequency distribution which can avoid the impact of frustration α by reaching perfect synchronization ($R = 1$) as well as it will create a broader explosive width in the presence of higher values of z.
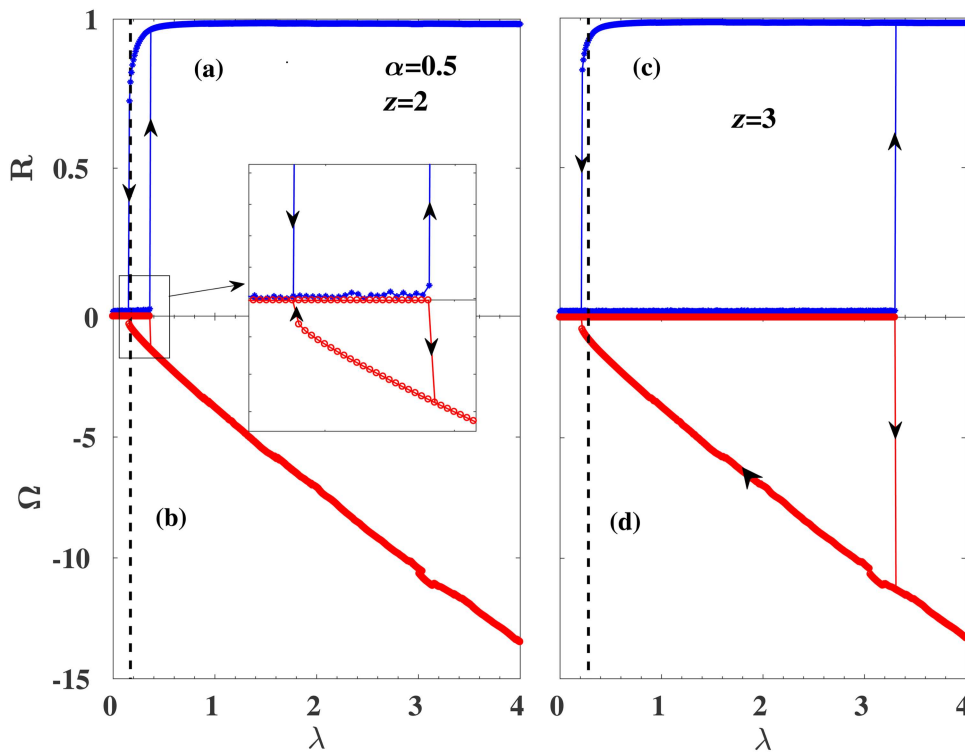
FIG. 3. Order parameter R and group angular velocity Ω as a coupling strength λ for two values of z. The blue curve indicates the synchronization diagram, and the red curve indicates the group angular velocity calculated from the model Eq. (1) for SF network of network size $N = 2000$, $\langle k \rangle = 12$, and $\gamma = 2.8$. The black dotted verticle line indicates the backward transition point of R and Ω calculated from the semi-analytic equations (A3) and (A4). All data are simulated with phase frustration $\alpha = 0.5$.
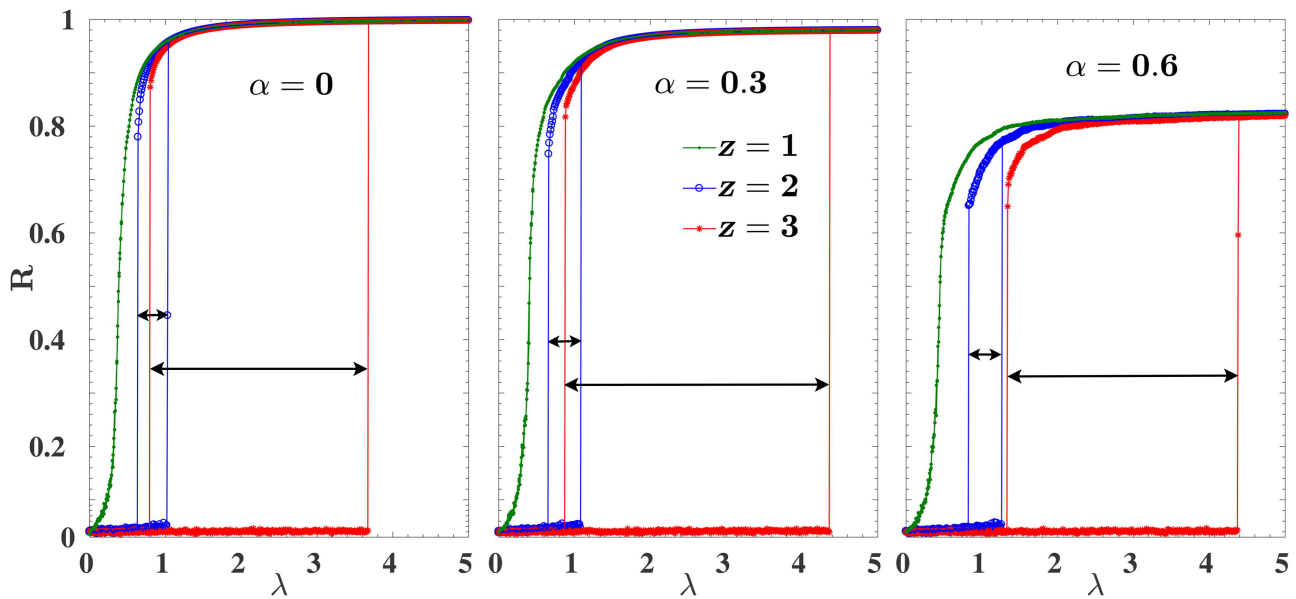
FIG. 4. ES and enhancement of a ES width in a small-world network. Impact of α and z is tested in Watts–Strogatz small-world network of size $N = 500$, $\langle k \rangle = 4$, and $\beta = 0.5$. The double headed arrow indicates the explosive width of the hysteresis transition.
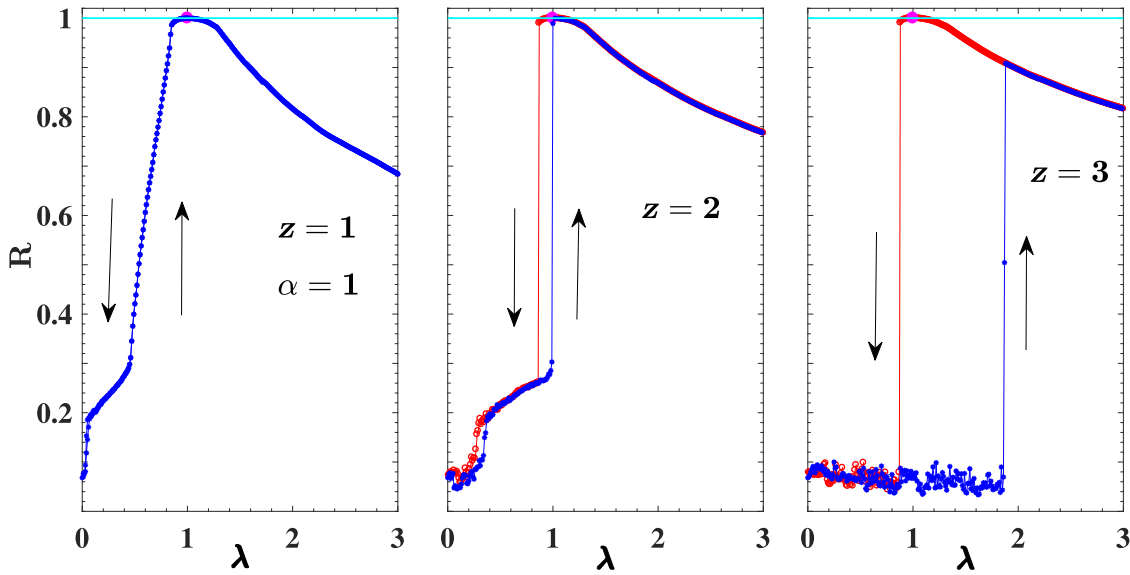
FIG. 5. Amplification of explosive width in the case of degree-frequency correlation. Order parameter R as a function of coupling strength λ for a SF network of network size $N = 2000$, $\langle k \rangle = 14$, and $\gamma = 2.8$ for different values of z. The blue line indicates the forward transition and the red line indicates the backward transition. The magenta dot on the cyan color line indicates our targeted point at $(1, 1)$.

III. AMPLIFICATION OF HYSTERESIS WIDTHS IN A DEGREE-FREQUENCY ENVIRONMENT

We have already shown that our adaptive strategy works efficiently when the frequencies are drawn from a Lorentzian distribution. A degree-frequency environment naturally induces ES;[15,33] however, a frustrated network ($\alpha > 0.3$[34]) cannot reveal ES even in the presence of degree-frequency correlated dynamics. Here, we seek to understand the impact of such coupling configurations in frustrated dynamics.

We consider a SF network of size $N = 2000$ with $\gamma = 2.8$ and average degree $\langle k \rangle = 14$, where the natural frequency of each oscillator scales with its own degree as $\omega_i = ak_i$, where a is a proportionality constant. We set the phase-frustration parameter $\alpha = 1$, and we take $a = \sin \alpha$. In this case, order parameter R does not exhibit the first-order transition for a non-adaptive environment ($z = 1$) (Fig. 5, shown in the left column with a blue line). Interestingly, one additional characteristic appears in the behavior of the order parameter, i.e., R approaching 1 at $\lambda = 1$. This is due to the emergence of perfect synchronization ($R = 1$)[35,36] for choosing a specific kind of frequency distribution.

As we know, in a perfect synchronization state, $\left| \theta_j - \theta_i \right| = 0$ and $R = 1$. Using Taylor's series approximation, Eq. (1) can be written as

$$\frac{d\theta_i}{dt} = \tilde{\omega}_i - \lambda \cos(\alpha) \sum L_{ij} \theta_j, \qquad (13)$$

where $\tilde{\omega}_i = \omega_i - \lambda \sin(\alpha) k_i$ and L is the Laplacian matrix. In a vector form, one can write $\dot{\theta} = \tilde{\omega} - \lambda \cos(\alpha) L\theta$. Assume that, in global synchronization, all the oscillators follow a common frequency Ω and if we consider a Ω rotating frame, the phases will be freezed in

this frame by setting themselves into steady states ($\frac{d\theta}{dt} = 0$). This further implies $\theta^* = \frac{L^\dagger \tilde{\omega}}{\lambda \cos(\alpha)}$, where $L^\dagger$ is the pseudo-inverse operator[37] of the Laplacian matrix L. Now if we choose $\omega_i = \sin(\alpha) k_i$ which sets $\tilde{\omega} = 0$ at $\lambda = 1$, and that eventually gives $\theta^* = 0$. This signifies that the frequency ensures perfect synchronization of oscillators ($R = 1$) at $\lambda = 1$ (magenta dot in each panel of Fig. 5 on the cyan line), although the choice of the higher value of $z (= 2)$ in R^{z-1} yields the explosive width (Fig. 5, middle panel). The hysteresis width is significantly increased for higher values of $z (= 3)$ (shown in the right panel). Therefore, we have shown that our adaptive strategy can create ES and enhance the ES width in these types of networks irrespective of the choice of the frequencies. The analytical prediction is confirmed in Fig. 5 assuring perfect synchronization at $\lambda = 1$, which also nullifies the contrarian effect of frustration parameter α. The forward line misses the perfect synchronization point (blue line), where the backward line coincides with $R = 1$ at $\lambda = 1$ for each case of z.

IV. CONCLUSIONS

We have investigated the phenomenon of explosive synchronization in complex networks of phase oscillators both numerically and analytically, based on an adaptive-coupling strategy. Numerical simulations for different networks in both frustrated and nonfrustrated environments show that, as a parameter (z) in the coupling function is tuned appropriately, networks undergo abrupt transition to (explosive) synchronization and width of the associated hysteresis loop is greatly enhanced. It is observed that the proposed strategy is quite general and is applicable for any type of networks and frequency distributions for the amplification of hysteresis widths. We

have confirmed that the strategy can successfully induce the emergence and enhancement of explosive synchronization in diverse frustrated environments. Based on the Ott–Antonsen ansatz, we have derived analytical expressions for the global order parameter and global frequency. The results obtained from the semi-analytical approach based on the Ott–Antonsen ansatz match with the backward transition points obtained from the numerical simulation of the entire complex networks.

APPENDIX: COUPLED EQUATION OF R AND Ω

The contribution of locked oscillators to the order parameter is

$$
R_l = \frac{(\cos\alpha - i\sin\alpha)}{\langle k \rangle} \int_{k_{\min}}^{\infty} \int kP(k)g(\omega)
$$
$$
\times \left[\sqrt{1 - \left(\frac{\omega-\Omega}{\lambda kR^z}\right)^2} + i\frac{\omega-\Omega}{\lambda kR^z} \right] dk\,d\omega H\left(1 - \left|\frac{\omega-\Omega}{\lambda kR^z}\right|\right).
$$
$$(A1)$$

Now, the contribution of drift oscillators to the order parameter is given by

$$
R_d = \frac{(\sin\alpha + i\cos\alpha)}{\langle k \rangle} \int_{k_{\min}}^{\infty} \int kP(k)g(\omega)\frac{\omega-\Omega}{\lambda kR^z}
$$
$$
\times \left[1 - \sqrt{1 - \left(\frac{\lambda kR^z}{\omega-\Omega}\right)^2} \right] dk\,d\omega H\left(\left|\frac{\omega-\Omega}{\lambda kR^z}\right| - 1\right).
$$
$$(A2)$$

Hence, we get $R = R_l + R_d$, where R_l and R_d are given by Eqs. (A1) and (A2), respectively. Now, comparing the real and imaginary parts, we get

$$
R\langle k \rangle = \cos\alpha \int_{k_{\min}}^{\infty} \int kP(k)g(\omega)\sqrt{1 - \left(\frac{\omega-\Omega}{\lambda kR^z}\right)^2} H
$$
$$
\times \left(1 - \left|\frac{\omega-\Omega}{\lambda kR^z}\right|\right) dk\,d\omega + \frac{\sin\alpha}{\lambda R^z}(\langle\omega\rangle - \Omega)
$$

$$
- \sin\alpha \int_{k_{\min}}^{\infty} \int kP(k)g(\omega)\frac{\omega-\Omega}{\lambda kR^z}\sqrt{1 - \left(\frac{\lambda kR^z}{\omega-\Omega}\right)^2} H
$$
$$
\times \left(\left|\frac{\omega-\Omega}{\lambda kR^z}\right| - 1\right) dk\,d\omega
$$
$$(A3)$$

and

$$
\langle\omega\rangle - \Omega = \lambda R^z\tan\alpha \int_{k_{\min}}^{\infty} \int kP(k)g(\omega)\sqrt{1 - \left(\frac{\omega-\Omega}{\lambda kR^z}\right)^2} H
$$
$$
\times \left(1 - \left|\frac{\omega-\Omega}{\lambda kR^z}\right|\right) dk\,d\omega + \int_{k_{\min}}^{\infty} \int P(k)g(\omega)(\omega-\Omega)
$$
$$
\times \sqrt{1 - \left(\frac{\lambda kR^z}{\omega-\Omega}\right)^2} H\left(\left|\frac{\omega-\Omega}{\lambda kR^z}\right| - 1\right) dk\,d\omega.
$$
$$(A4)$$

By solving the above two equations, we can get the set of values for order parameter R corresponding to coupling strength λ.

REFERENCES

[1] T. Aoki and T. Aoyagi, Phys. Rev. Lett. **102**, 034101 (2009).
[2] S.-Y. Ha, S. E. Noh, and J. Park, SIAM J Appl. Dyn. Syst. **15**, 162–194 (2016).
[3] D. V. Kasatkin and V. I. Nekorkin, Eur. Phys. J. Spec. Top. **227**, 1051–1061 (2018).
[4] A. C. Kalloniatis and M. Brede, Phys. Rev. E **99**, 032303 (2019).
[5] M. Chen, Y. Shang, C. Zhou, Y. Wu, and J. Kurths, Chaos **19**, 013105 (2009).
[6] S. Chakravartula, P. Indic, B. Sundaram, and T. Killingback, PLoS ONE **12**, e0178975 (2017).
[7] R. K. Niyogi and L. Q. English, Phys. Rev. E **80**, 066213 (2009).
[8] P. S. Skardal, D. Taylor, and J. G. Restrepo, Phys. D **267**, 27–35 (2014).
[9] M. Li, S. Guan, and C.-H. Lai, New J. Phys. **12**, 103032 (2010).
[10] P. Khanra, P. Kundu, C. Hens, and P. Pal, Phys. Rev. E **98**, 052315 (2018).
[11] A. Kachhvah and S. Jalan, Euro Phys. Lett. **119**, 60005 (2017).
[12] M. M. Danziger, I. Bonamassa, S. Boccaletti, and S. Havlin, Nat. Phys. **15**, 178–185 (2019).
[13] M. M. Danziger, O. I. Moskalenko, S. A. Kurkin, X. Zhang, S. Havlin, and S. Boccaletti, Chaos **26**, 065307 (2016).
[14] R. S. Pinto and A. Saa, Phys. Rev. E **92**, 062801 (2015).
[15] J. Gomez-Gardeñes, S. Gomez, A. Arenas, and Y. Moreno, Phys. Rev. Lett. **106**, 128701 (2011); P. Ji, T. Peron, P. J. Menck, F. A. Rodrigues, and J. Kurths, Phys. Rev. Lett. **110**, 218701 (2013).
[16] S. Boccaletti, J. A. Almendral, S. Guan, I. Leyva, Z. Liu, I. Sendiña-Nadal, Z. Wan, and Y. Zou, Phys. Rep. **660**, 1–94 (2016).
[17] I. Leyva, A. Navas, I. Sendiña-Nadal, J. A. Almendral, J. M. Buldu, M. Zanin, D. Papo, and S. Boccaletti, Sci. Rep. **3**, 1281 (2013); Y. Zou, T. Pereira, M. Small, Z. Liu, and J. Kurths, Phys. Rev. Lett. **112** 114102 (2014).
[18] G. Filatrella, N. F. Pedersen, and K. Wiesenfeld, Phys. Rev. E **75**, 017201 (2007).
[19] X. Zhang, S. Boccaletti, S. Guan, and Z. Liu, Phys. Rev. Lett. **114**, 038701 (2015).
[20] Y. Kuramoto, *Chemical Oscillations, Waves, and Turbulence* (Springer, New York, 1984).
[21] J. A. Acebròn, L. L. Bonilla, C. J. P. Vicente, F. Ritort, and R. Spigler, Rev. Mod. Phys. **77**, 137–185 (2005).
[22] F. Dörfler and F. Bullo, SIAM J. Control Optim. **50**(3), 1616–1642 (2012).
[23] F. A. Rodrigues, T. K. D. M. Peron, P. Ji, and J. Kurths, Phys. Rep. **610**, 1–98 (2016).
[24] H. Sakaguchi and Y. Kuramoto, Prog. Theor. Phys. **76**, 576 (1986).
[25] O. E. Omel'chenko and M. Wolfrum, Phys. Rev. Lett. **109**, 164101 (2012).
[26] M. A. Lohe, Automatica **54**, 114–123 (2015).

[27] P. S. Skardal, D. Taylor, J. Sun, and A. Arenas, Phys. Rev. E **91**, 010802(R) (2015).

[28] P. S. Skardal, D. Taylor, J. Sun, and A. Arenas, Phys. D Nonlinear Phenom. **323**, 40–48 (2016).

[29] E. Ott and T. M. Antonsen, Chaos **18**, 037113 (2008).

[30] T. K. D. Peron and F. A. Rodrigues, Phys. Rev. E **86**, 016102 (2012).

[31] T. Ichinomiya, Phys. Rev. E **70**, 026116 (2004).

[32] S. N. Dorogovtsev, A. V. Goltsev, and J. F. F. Mendes, Rev. Mod. Phys. **80**, 1275 (2008).

[33] B. C. Coutinho, A. V. Goltsev, S. N. Dorogovtsev, and J. F. F. Mendes, Phys. Rev. E **87**, 032106 (2013); S. Yoon, M. Sorbaro Sindaci, A. V. Goltsev, and J. F. F. Mendes, Phys. Rev. E **91**, 032814 (2015).

[34] P. Kundu, P. Khanra, C. Hens, and P. Pal, Phys. Rev. E **96**, 052216 (2017).

[35] P. Kundu, C. Hens, B. Barzel, and P. Pal, Europhys. Lett. **120**, 40002 (2018).

[36] M. Brede and A. C. Kalloniatis, Phys. Rev. E **93**, 062315 (2016).

[37] A. Ben-Israel and T. N. E. Greville, *Generalized Inverses Theory and Applications*, 2nd ed. (Canadian Mathematical Society, Springer, 2002).